ISSN: 0067-2904

Synthesis, Characterization and Biological Evaluation of Polymer Nano Dimetal Oxides Derived from Poly Methylmetha Acrylate and Y_2O_3 \ La_2O_3 Prepared in Green Method

Zainab Ahmed Abd*, Nada Mutter Abbass
Department of Chemistry, College of Science, University of Baghdad, Baghdad, Iraq

Received: 9/2/2024 Accepted: 18/9/2024 Published: 30/10/2025

Abstract

In this work, metal oxides [Y_2O_3\$La_2O_3$] nanoparticles were synthesized using a green method with ashwagandha extract, which served as a reducing agent. This extract also catalyzed the polymerization of poly methylmetha acrylate, resulting in the formation of nanocomposites [PMMA\$Y_2O_3$\$La_2O_3$]. The morphology, size, and structures of the synthesized nanocomposites were determined and characterized using thermogravimetric analysis (TGA), x-ray diffraction (XRD), differential scanning calorimetry (DSC) analysis, and field emission scanning electron microscopy (FESEM), tested by antioxidant activity and antibacterial activity. To confirm the design of nanocomposites-based nanostructures and to reveal unique characteristics, the distribution of the nanoparticles within PMMA was analyzed determined. The results from AFM of the synthesized nanostructure of Y_2O_3 and La_2O_3, showed that the size of NPs was within the nanoscale range. The biological activities of synthesized nanocomposites were examined, including antioxidant and the use of these nanocomposites as inhibitors for bacteria. The findings demonstrated that the nanocomposites revealed they have a significant inhibitory effect.

Keywords: Polymer composite, Poly Methylmetha Acrylate, Yttrium Oxide, Lanthanum Oxide, SEM, Antioxidant Activity, Antibacterial Activity

تخليق وتوصيف وتقييم بايولوجي لأكاسيد بوليمر النانو للمعادن الثنائية المحضرة من الأكريلات متعددة الميثيل و Y_2O_3 \ La_2O_3 بواسطة طريقة خضراء

زينب احمد عبد*, ندى مطير عباس
قسم الكيمياء, كلية العلوم, جامعة بغداد, بغداد, العراق

الخلاصة

في هذا العمل، تم تخليق جزيئات نانوية لأكاسيد المعادن في هذا العمل، تم تخليق جزيئات نانوية لأكاسيد المعادن [Y_2O_3\$La_2O_3$] باستخدام طريقة صديقة للبيئة بواسطة مستخلص الأشواغاندا، الذي عمل كعامل مختزل. كما قام هذا المستخلص بتحفيز بلمرة بولي ميثيل ميثاكريلات (PMMA)، مما أدى إلى تشكيل المواد النانوية المركبة [PMMA\$Y_2O_3$\$La_2O_3$]. تم تحديد وتحليل الشكل الخارجي، الحجم، والهياكل للمواد النانوية المركبة المُصنّعة باستخدام التحليل الحراري الوزني (TGA)، حيود الأشعة السينية (XRD)، التحليل بالمسح

*Email: zainabahmeddd8@gmail.com

الحراري التفاضلي (DSC)، وميكروسكوب الإلكترون الماسح ذو الانبعاث الميداني (FESEM)، بالإضافة إلى اختبار النشاط المضاد للأكسدة والنشاط المضاد للبكتيريا. لتأكيد تصميم الهياكل النانوية القائمة على المواد النانوية المركبة وكشف الخصائص الفريدة، تم تحليل توزيع الجزيئات النانوية داخل PMMA. أظهرت نتائج الميكروسكوب الذري (AFM) للهياكل النانوية المُصنّعة من Y_2O_3 و La_2O_3 أن حجم الجزيئات النانوية كان ضمن النطاق النانوي. تم فحص الأنشطة البيولوجية للمواد النانوية المركبة المُصنّعة، بما في ذلك النشاط المضاد للأكسدة واستخدام هذه المواد كمثبطات للبكتيريا. أظهرت النتائج أن المواد النانوية المركبة لها تأثير مثبط كبير.

1. Introduction

A nanocomposite is described as a composite material that incorporates a phase with a nanoscale dimension. It can encompass nanoparticles, nanotubes, or layered nanostructures [1, 2]. Due to their composition of multiple stages, those materials are taken into consideration as a couple of levels substances with at the least one in all phases having a diameter in the variety of 10 and 100 nm [3]. Nanocomposites have emerged as useful alternatives to engineering substances that possess obstacles [4]. Nano composites may be divided into different types based totally at the factors in their scattered matrix and dispersion segment[5] .

Numerous new substances with unique capabilities were made possible by way of this speedy developing quarter [6]. In addition to showing attributes from the constituent substances, nanocomposites also can display novel qualities because of their distinct structure and nanoscale interactions [7]. Numerous investigations had been done at the optical and electrical houses of nanocomposites, which locate substantial use in numerous programs which include photo catalysis and sensors [8]. Biomedical implants and catheters are among the many makes use of for PMMA\$Y_2O_3$\$La_2O_3$] NPs, that have additionally shown antibacterial pastime. Antibacterial activity is also established by using [PMMA$Y_2O_3La_2O_3$] NPs [9]. Y_2O_3 is broadly used as a number host for various rare earth dopants, photodynamic remedy, and biological imaging [10]. It has also been used inside the optoelectronic disciplines for cancer therapy, biosensors, and bioimaging as a polarizer, phosphor, and laser host cloth. Because of their antibacterial and antioxidant properties, Y_2O_3 NPs are intriguing [9]. Withania somnifera, the scientific call for ashwagandha, is an herb indigenous to Asia and Africa. Known by means of many as "Indian ginseng," this herb has been used for heaps of years in ancient Indian Ayurvedic medication to treat a number situations, which include ache and infection, insomnia, and dietary enhancement [11].

The study aims to investigate the SEM characteristics, antibacterial, and antioxidant properties of [PMMA\$Y_2O_3$\$La_2O_3$]. To achieve this, we developed a simple green technique for yttrium and lanthanum synthesis and conducted various laboratory-based antibacterial tests. The disc diffusion method was employed to establish the inhibitory impact of nanocomposites direct on reference strain cultures of *Escherichia coli* (-) and *Staphylococcus aurous* (+) gram positive bacteria. Additionally, antioxidant and Sem effects were reviewed.

2. Materials and Methods

2.1 Materials

Poly methylmetha acrylate, ashweghanda extract solution**,** Y_2O_3 yttrium oxide, La_2O_3 lanthanum oxide, LaCl3.6H2O where supplied form (BDH, UK).

2.2 Methods

2.2.1 Preparation of Ashweghanda Aqueous Extract [12]:

Typically, 4 gm of Ashwagandha extract are mixed with 150 mL of distilled water. The mixture was then heated and stirred for 15 minutes. After that period, the liquid is strained to prepare it for subsequent synthesis.

2.2.2 Yttrium Oxide (Nps) Synthesis Using a Green Technique [13]:

Four grams of Ashwagandha extract were dissolved in 100 mL of distilled water. The solution was heated at 80°C for 15 min, then filtered to remove any residues. Simultaneously, 6 gm of Y_2O_3 (with a particle size of approximately 110 nm) were added to 250 mL of distilled water. This mixture was also heated at 80°C and stirred for 15 min. Subsequently, the Y_2O_3 solution was treated dropwise with Ashwagandha extract until the solution turned brown instead of white. After that, the mixture was heated to 100°C in order to evaporate the solvent entirely. The resulting solution was allowed to cool to ambient temperature after drying at 60°C, which caused a precipitate to form.

2.2.3 Lanthanum Oxide (Nps) Synthesis Using a Green Technique [13]:

One hundred milliliters of distilled water were mixed with 4 gm of ashwagandha extract. After 15 min of heating the solution to 80°C, any leftovers were filtered out. At the same time, 250 mL of distilled water were used to dissolve 6 gm of $LaCl_3 \cdot 6H2O$. After being heated to 80°C, this mixture was stirred for 15 min. The Ashwagandha extract was then added dropwise to the $LaCl_3 \cdot 6H2O$ solution while stirring, resulting in a color change from white to brown. The mixture was subsequently heated at 100°C to completely evaporate the solvent. After drying at 60°C, the solution was allowed to cool to room temperature, leading to the formation of a precipitate.

2.2.4 Preparation of PMMA/Y_2O_3/La_2O_3 Nanocomposites [14]:

To 1 gram of polystyrene, which serves as the ligand, 25 mL of acetone (C_3H_6O) was add and the mixture was refluxed 1 hour at 50°C, yielding solution A. Simultaneously, disperse 0.1 gm of Y_2O_3 NPs and 0.1 grams of La_2O_3 NPs in 10 mL of acetone. This mixture was then subjected to ultrasonic agitation for 5 min, producing solution B. Following this, solution B is added to solution A, and the combined mixture is then subjected to reflux for an additional 5 hours. The resulting mixture is subsequently collected and permitted to solidify at ambient temperature.

3. Results and Discussion

3.1 Atomic Force Microscopy (AFM) for Yttrium Oxide Nanocomposites

AFM offers a resolution of fractions of Angstrom, which is more than 1000 times greater in comparison with the standard optical microscope. AFM uses a micro- and nanoscale cantilever to scan the specimen surface at the nanoscale level. The cantilever has a sharp tip (probe) made of silicon or silicon nitrite at the end [15]. AFM images in two dimensions (2D) and three dimensions (3D) view of metal oxide nanocomposites, which reveals the topography, particles distribution and average diameter for the nanocomposites synthesized via (green method), the Y_2O_3 nanostructure shown that the particles' average diameter was 170.9 nm [16].

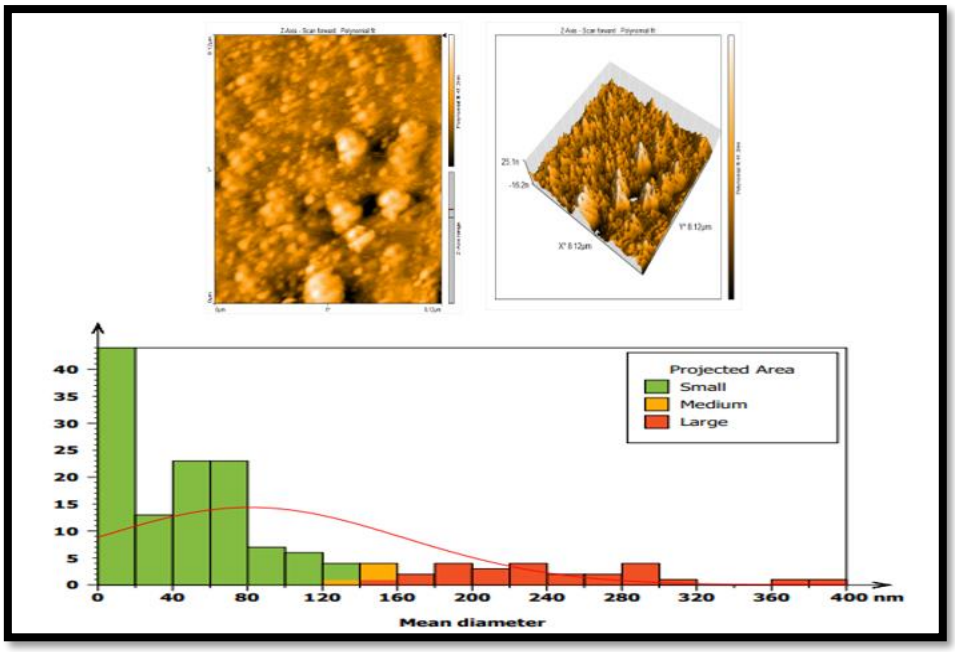

Figure 1: 2D and 3D AFM images of Y_2O_3 nanoparticles.

3.2 Atomic Force Microscopy (AFM) fpr Lanthanum Oxide Nanocomposites:

AFM images, presented in both two dimensions (2D) and three dimensions (3D) views, provide insights into the topography, particles distribution and average diameter of metal oxide [Y_2O_3] nanostructure synthesized via (green method). The analysis revealed that average diameter was 268.6 nm [17].

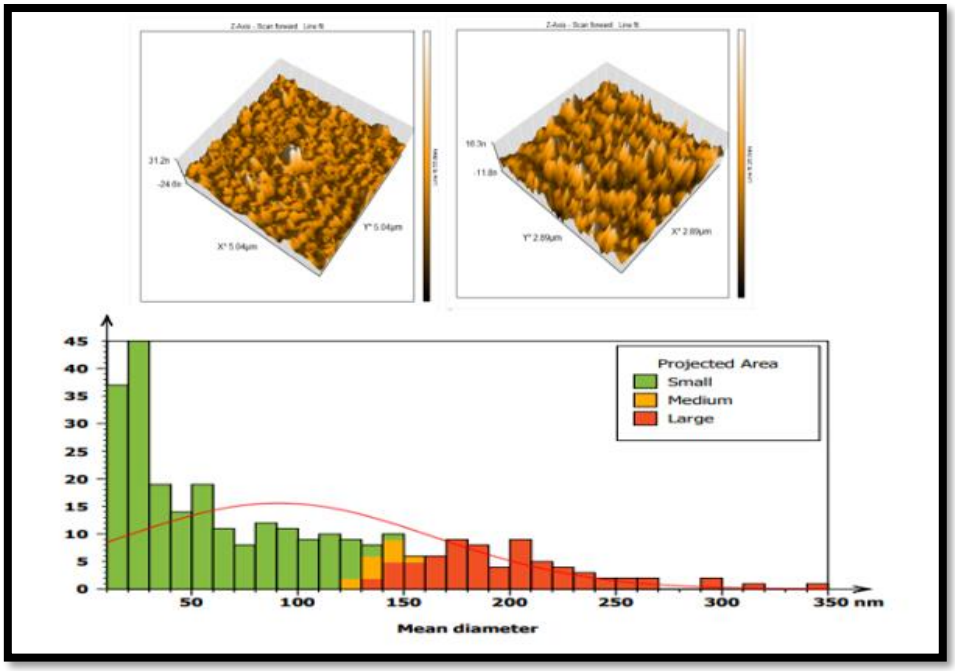

Figure 2: 2D and 3D AFM images of La_2O_3 nanoparticles.

3.3 Field Emission Scanning Electron Microscopy of (PMMA\$Y_2O_3$\$La_2O_3$) Nanocomposites

Field-emission microscopy (FEM) is an analytical method used to examine needle apex surfaces. Erwin Wilhelm Müller created the FEM in 1936 [18]. This measurement revealed

two distinct nanostructures: irregular sphere-like nanostructures with diameters ranging from 20.10 to 62.88 nm, cloud-shaped nanoparticles with a thickness of about 3.6 nm, and sheet-like nanoparticles. These nanostructures indicate that the prepared nanocomposites are on the nanoscale. As shown in Figure 3.

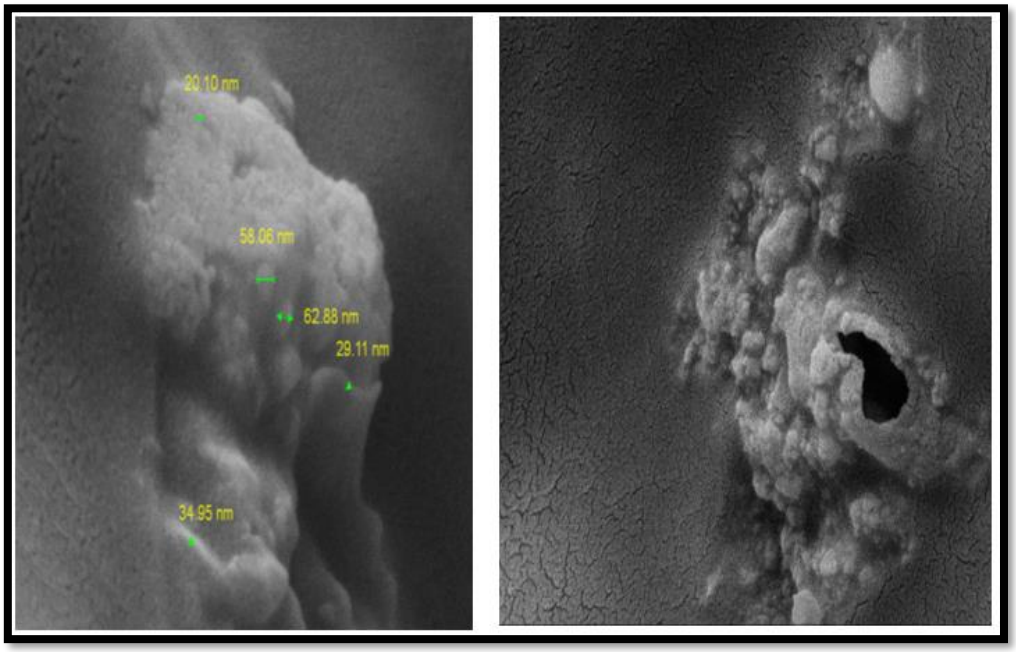

Figure 3: FE-SEM of (PMMA/ Y_2O_2/ La_2O_3) nanocomposites.

3.4 X-Ray Diffraction of (PMMA\ Y_2O_3 \ La_2O_3) Nanocomposite

An essential and popular method for characterizing materials is X-ray diffraction, or XRD [19]. XRD pattern of [PMMA/Y_2O_2/La_2O_3] nanostructure has peaks exhibited diffraction at the 2θ values (14°, 29°, 34°,36°, 40°,41°, 43°,48,50° and 53°). Standard JCPDS card number (00-040-0133), however, mean particle size for [PMMA/Y_2O_2/ La_2O_3] nanoparticles have crystal size of 20.01 nm.

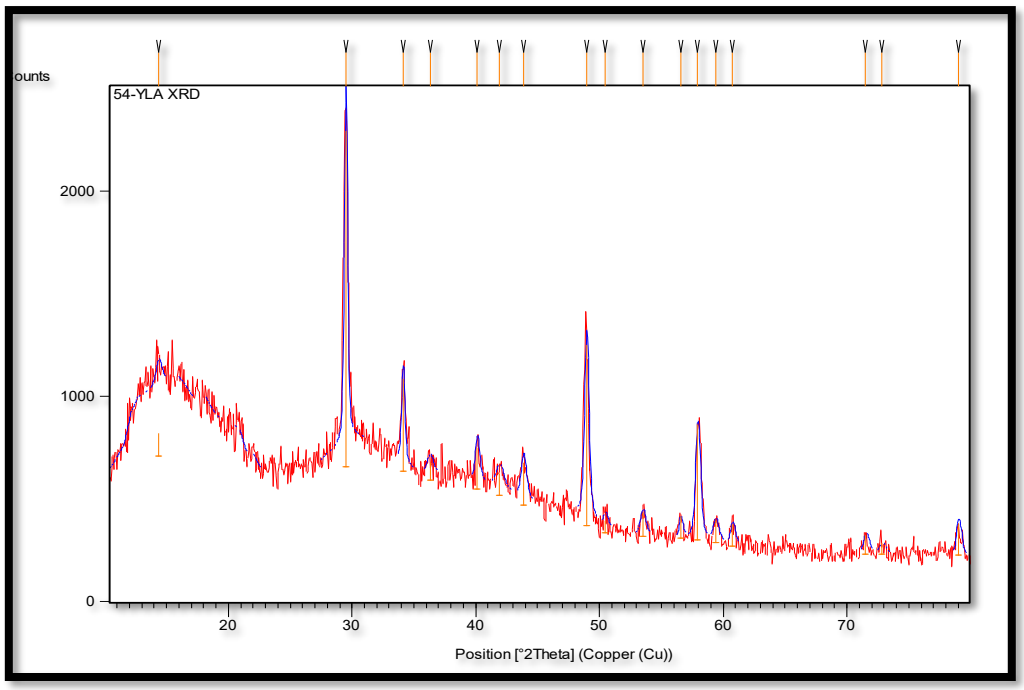

Figure 4: X-ray diffraction (XRD) pattern of [PMMA/ Y_2O_3/ La_2O_3] nanocomposites.

3.5 Thermogravimetric Analysis (TGA) of (Y_2O_3/ La_2O_3) Nanocomposites

TGA of synthesized nanocomposites showed four stages of weight loss [20]:

1. First stage: with a weight loss percentage of 8.438%, is observed due to physical adsorption of water onto the nanocomposites because of the high surface area of the nanomaterial. This occurs at temperatures between 35 and 120 °C.
2. The second stage occurs between 120 and 440 °C, and the third stage occurs between 440 and 800 °C. During these stages, a cumulative weight loss of 55.39% occurs during these stages, which also involve the beginning of the loss of acrylate units and the breakdown of the polymer's carbon backbone.
3. Fourth stage: at a temperature of more than 800 °C and a weight (percentage) of 12.18%, this stage is thought to be a good indicator of the reaction's success and may be related to the quantity of Y_2O_3 and La_2O_3 NPs residue. See Table 1 for more information.

Table 1: Show all stage decompositions for (PMMA/ Y_2O_3/ La_2O_3) nanocomposites.

Ser	*Stage (temp) °C*	*Loss wt %*	*Loss wt % (theoretical)*	*status*
1	35-120	8.438	9	Water loss
2	120-440	22.54	23	beginning of the acrylate unit's loss
3	440-800	32.85	33	Breakdown of the carbon skeleton
4	More than 800	12.18	13	remnant of metal and metal oxide

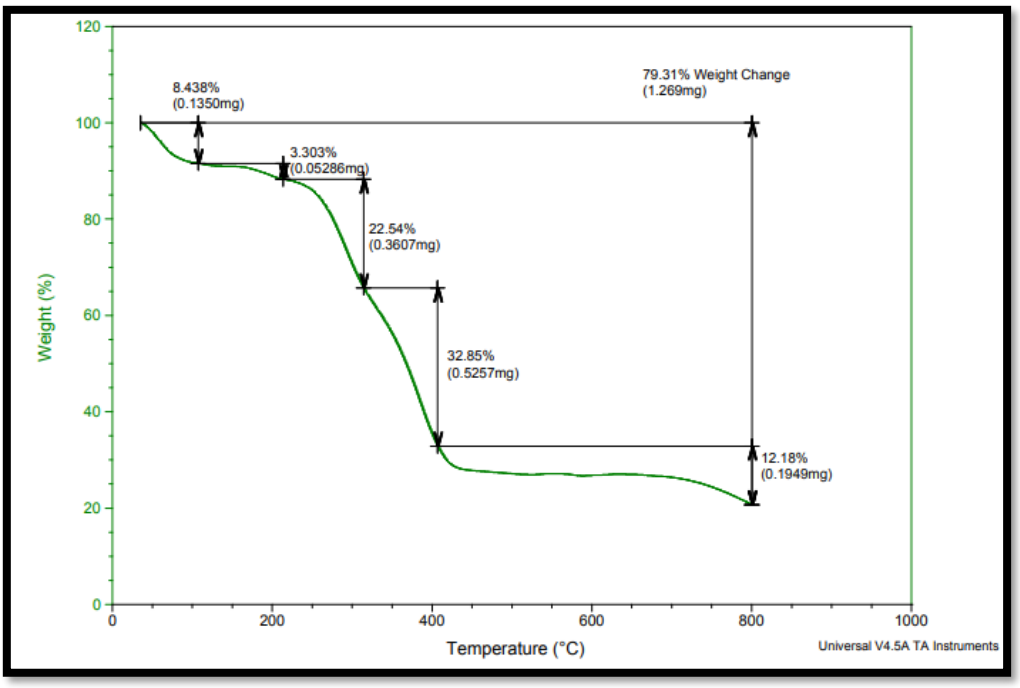

Figure 5: TGA of (PMMA/ Y_2O_3/ La_2O_3) nanocomposites.

3.6 Differential Scanning Calorimetry of (PMMA/ Y_2O_3/ La_2O_3) Nanocomposites.

The thermal analysis technique known as differential scanning calorimetry (DSC) measures the amount of energy that a sample can absorb or release as heat capacity. DSC equipment can be used to determine the phase diagram, entropy, enthalpy, and thermal capacity[21]. The produced (PMMA/Y_2O_3/La_2O_3) nanocomposites underwent two endothermic stages of calorimetry (DSC) analysis. First, at 382.81°C, which is equivalent to ampere-hour (AH) to

2756 J/g for (PMMA/Y_2O_3/La_2O_3) nanocomposites, it is considered that PMMA in nanocomposites has reached its glass transition temperature when compared to a standard reference of 100°C. It is acknowledged that PMMA in nanocomposites has reached its melting point when compared to a standard reference of 270 °C. This further demonstrates the effectiveness of the response, as seen in Figure 6.

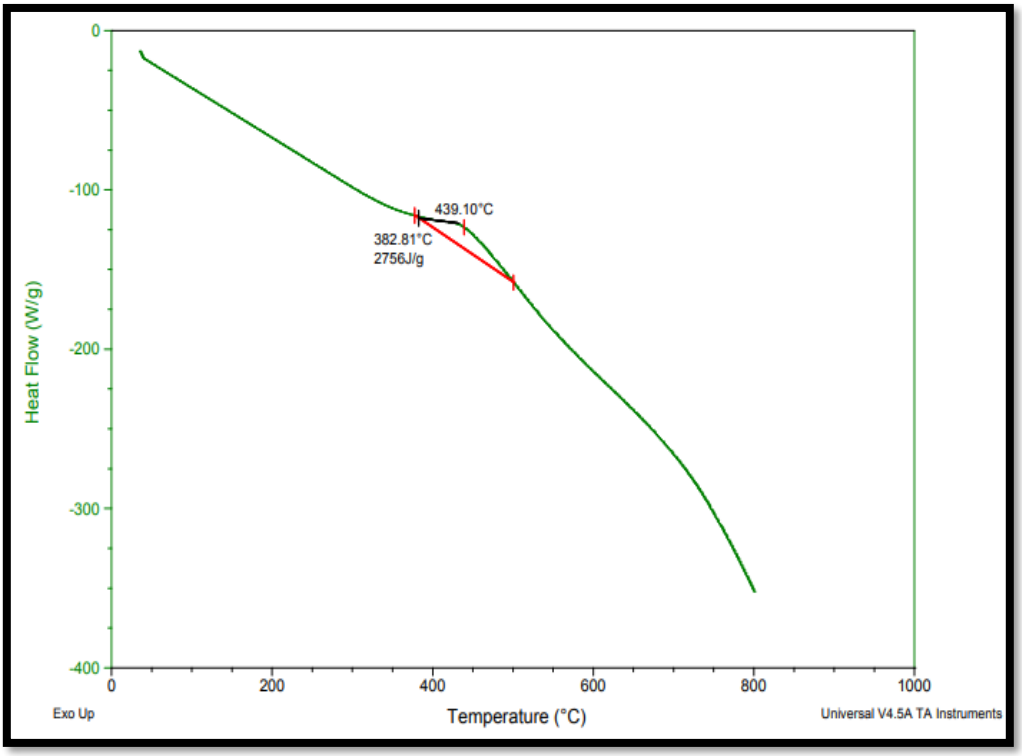

Figure 6: DSC of (PMMA/ Y_2O_3/ La_2O_3) nanocomposites.

4. Biological Evaluation

4.1 Antioxidant of (PMMA/ Y_2O_3/ La_2O_3) Nanocomposites

A. Solutions [22]

- DPPH (1,1-Diphenyl-2-picryl-hydrazyl): 4.3 mg of DPPH was dissolved in 3.3 mL of DMSO-methanol (1:9 v/v), and the test tubes were covered with aluminum foil to keep the solution dark.
- Plant extract: Four concentrations (0.0625, 0.125, 0.250 and 0.500 mg/ mL) were prepared by dissolving the required weight of methanolic extract in 1-2 drops of DMSO, and then the volume was made-up with distilled water.
- Ascorbic acid (vitamin C): Similar concentrations of the plant extract were prepared.

B. Method

Using the Sanja et al. (2009) approach [22], the antioxidant activity of the plant methanolic extract and standard (vitamin C) was evaluated based on the stable DPPH free radical's ability to scavenge radicals. To 3.9 mL of DPPH solution in a test tube, an aliquot of 0.1 mL of the extract or standard (0.625, 0.125, 0.250, and 0.500 mg/ mL) was added. Using a spectrophotometer, the absorbance of each solution was measured at 517 nm following a 30-minute incubation period at 37°C. Three duplicates of each measurement were taken. The Eq. (1) was used to determine the DPPH radical's scavenging capacity:

$$\text{DPPH radical scavenging activity}\,(\%) = \left(1 - \frac{\text{Absorbance of Sample}}{\text{Absorbance of Standard}}\right) \times 100 \qquad (1)$$

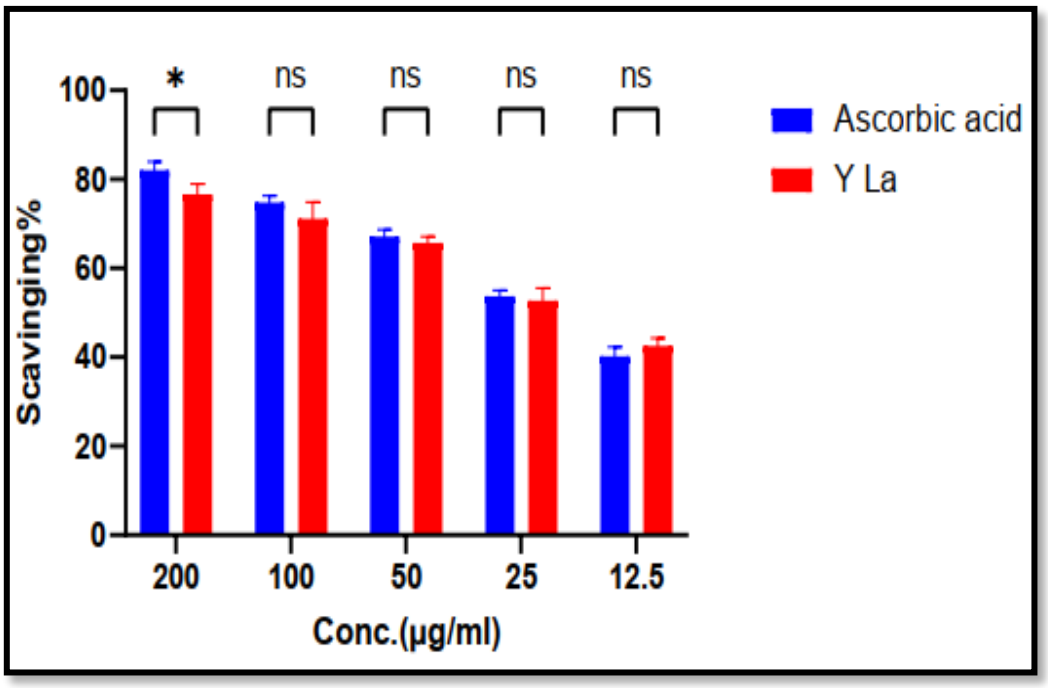

Figure 7: Antioxidant of (PMMA/ Y_2O_3/ La_2O_3) nanocomposites.

4.2 Antibacterial Activity of (PMMA/ Y_2O_3/ La_2O_3) Nanocomposites

The study evaluated the antibacterial efficacy of the nanocomposites against various bacterial strains, including *E. coli (G-), S. aureus (G+), Pseudomonas (G-), and Streptococcus (G+)*. As evident from Figure 8 and Table 2, the nanocomposites demonstrated significant antibacterial activity, inhibiting bacterial growth to a greater extent than the control, Amoxicillin. To understand the contribution of each component of the nanocomposites to this biological activity, it is essential to analyze the underlying mechanisms.

Contribution of Nanocomposite Components

Production of Free Radicals: The nanocomposites are shown to produce free radicals through various mechanisms such as photocatalysis, redox reactions, thermal decomposition, and surface interactions. These free radicals interact with bacterial cells, causing oxidative stress and damage to critical cellular components including proteins, DNA, and cell membranes.

Mechanisms:

- Photocatalysis: By absorbing light, nanocomposites can produce electron-hole pairs that cause reactive oxygen species (ROS) to develop. The cell structures of bacteria can be harmed by these ROS.
- Redox procedures: By promoting redox techniques that result in radicals, the nanocomposites can put microorganism underneath oxidative stress.
- Thermal degradation: The nanocomposites might also break down and launch radicals whilst heated.
- Surface Interactions: Through surface -mediated interactions, the interaction of bacterial cells with nanocomposite surfaces can result in the manufacturing of ROS.
- Evidence: Similar methods wherein nanomaterials produce ROS that have an impact on microbial cells have been identified in preceding studies, which includes those carried out by means of Smith and co-workers (2021) [23] as well as Johnson and co-workers (2022) [24].

Electrostatic Interactions: Metal oxides such as Y_2O_3 as well as La_2O_3 discovered inside the nanocomposites launch charged metallic ions. These ions bond electrostatically to the negatively charged bacterial mobile membranes. The disruption of membrane characteristic as a consequence of this interplay increases the risk of oxidative pressure and membrane harm.

Mechanisms:

- Electrostatic Binding: The bacterial cell membrane's negatively charged components bind to charged metallic ions (positively) from the nanocomposites, increasing the membrane's permeability and ensuing in leakage.
- Enhanced Oxidative Stress: The bacterial cellular harm due to metallic ion binding might be amplified via oxidative pressure.
- Evidence: These electrostatic interactions are regarded to aggravate oxidative stress, as suggested by using Kim and co-workers (2007) [25]. Our is in line with the antibacterial effects that have been discovered in our research.

Theoretical Implications

The new observe ads to our knowledge of ways various nanocomposites' constituent parts affect their biological activity. It emphasizes the critical roles that electrostatic interactions and the manufacturing of free radicals play. A crucial contribution to our know-how is that nanocomposites' better antibacterial activities end result from their potential to generate unfastened radicals and engage with bacterial mobile membranes thru electrostatic forces. The present look at validates and extends standard theories by way of contrasting its results with other investigations, which includes those on the photocatalytic and electrostatic characteristics of nanomaterials. This offers critical new statistics for refining the composition of nanocomposite materials to improve their antibacterial properties.

Table 2: The ability of (PMMA/Y_2O_3/La_2O_3) nanocomposites to inhibit microorganisms.

Bacterial Strain	*PMMA/ Y_2O_3/ La_2O_3 (µg/mL)*	*Effect*
E. coli (G-)	100 µg/mL	Significant inhibition
	250 µg/mL	Moderate inhibition
	500 µg/mL	Minimal inhibition
S. aureus (G+)	50 µg/mL	Significant inhibition
	100 µg/mL	Moderate inhibition
	200 µg/mL	Minimal inhibition
pseudomonas (G-)	150 µg/mL	Significant inhibition
	300 µg/mL	Moderate inhibition
	600 µg/mL	Minimal inhibition
streptococcus (G+)	75 µg/mL	Significant inhibition
	150 µg/mL	Moderate inhibition
	300 µg/mL	Minimal inhibition

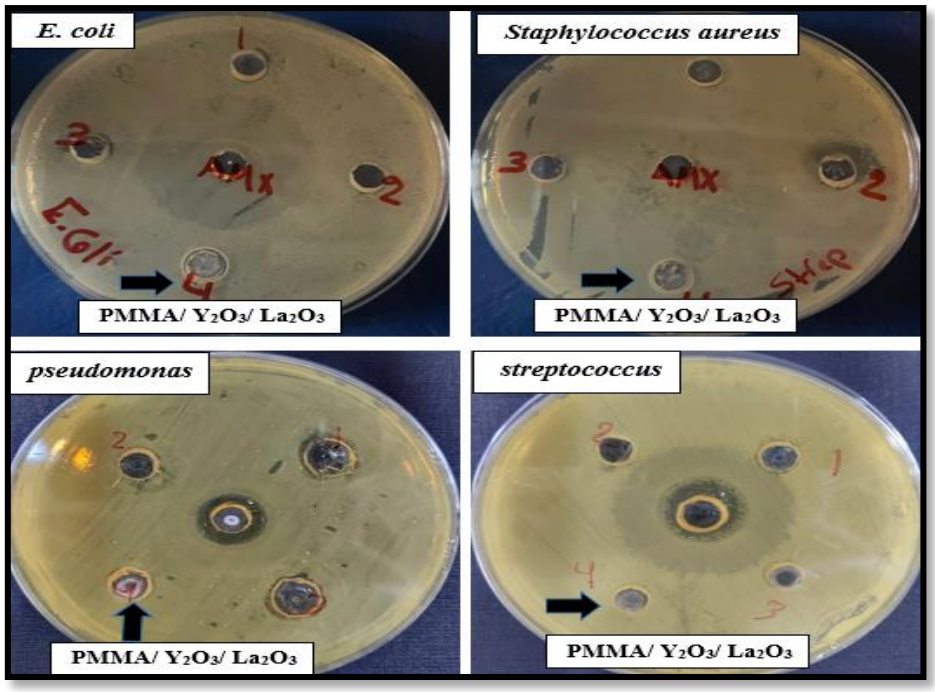

Figure 8: Antibacterial activity of (PMMA/ Y_2O_3/ La_2O_3) nanocomposites on the bacteria *E. coli, Staphylococcus aureus, pseudomonas*, and *streptococcus* demonstrated that nanocomposites.

Conclusion

Yttrium as well as lanthanum oxide nanorods and ashweghanda extract answer had been applied to synthesis the Poly methylmetha acrylate [Y_2O_3\ La_2O_3] nanocomposites. Subsequently, the nanocomposite changed into formed through blending it with polymethyl methacrylate (PMMA) that were dissolved in acetone. The composite become synthesised as nanoparticles, with dimensions and particle sizes of much less than one hundred nm, in keeping with the outcomes of the AFM technique measurements. Additionally, XRD checking out found out that metal nanoparticles developed as a coating layer over and between polymethyl methacrylate, and PMMA nanoparticles have a cubic structure. Knowing that microorganisms can slow down their growth, researchers looked into the antibacterial and antioxidant properties. After measuring the antioxidant activity against free radicals, a satisfactory scavenging ratio was obtained (the concentration of a certain pollutant in precipitation divided by the concentration of the pollutant in air).

Acknowledgment

The authors appreciate the cooperation of the teaching staff in the Department of Chemistry, College of Science, University of Baghdad.

Conflict of Interest

There are no conflicts of interest.

Funding

There is no funding for the article.

References

[1] S. Ganeshkumar, A. Kumar, J. Maniraj, Y. S. Babu , A. K. Ansu , A. Goyal, I. K. Kadhim, K. K. Saxena, C. Prakash, R. Altuijri, M. I. Khan, and A. M. Hassan, "Exploring the potential of nano

technology: a assessment of nano-scale multi-layered-composite coatings for cutting tool performance," *Arabian Journal of Chemistry,* vol. 16, no. 10, p. 105173, 2023.

[2] Z. A. Latif, A. M. Mohammed, and N. M. Abbass, "Synthesis and characterization of polymer nanocomposites from methyl acrylate and metal chloride and their application," *Polymer Bulletin,* vol. 77, pp. 5879-5898, 2020.

[3] C. P. Goh and W. C. Tan, "Analysis of the Nano-composite Column using Static and Dynamic Methods," *Journal of Innovation and Technology,* vol. 2023, no. 29, pp. 1-9, 2023.

[4] Z. Almarbd and N. M. Abbass, "Synthesis and characterization of TiO2, Ag2O, and graphene oxide nanoparticles with polystyrene as a nonocomposites and some of their applications," *Eurasian Chemical Communications,* vol. 4, pp. 1033-1043, 2022.

[5] J. Wang, J. Y. Yang, I. M. Fazal, N. Ahmed, Y. Yan, H. Huang, Y. Ren, Y. Yue, and S. Dolinar, "Terabit free-space data transmission employing orbital angular momentum multiplexing," *Nature photonics,* vol. 6, no. 7, pp. 488-496, 2012.

[6] K. Khan, A. K. Tareen, M. Aslam, R. Wang, Y. Zhang, A. Mahmood, Z. Ouyang, H. Zhang, and Z. Guo, "Recent developments in emerging two-dimensional materials and their applications," *Journal of Materials Chemistry C,* vol. 8, no. 2, pp. 387-440, 2020.

[7] M. R. Abdel-Salam, G. Ge, M. Fauchoux, R. W. Besant, and C. J. Simonson, "State-of-the-art in liquid-to-air membrane energy exchangers (LAMEEs): a comprehensive review," *Renewable and Sustainable Energy Reviews,* vol. 39, pp. 700-728, 2014.

[8] B. Aldabbagh, H. Jawad, and R. Mahdi, "Study of the properties of MgO/Poly methyl methacrylate Nano-composites," in *Journal of Physics: Conference Series*, 2021, vol. 2114, no. 1: IOP Publishing, p. 012039.

[9] G. Rajakumar, L. Mao, T. Bao, W. Wen, S. Wang, T. Gomathi, N. Gnanasundaram, and M. Rebezov, "Yttrium oxide nanoparticle synthesis: an overview of methods of preparation and biomedical applications," *Applied Sciences,* vol. 11, no. 5, p. 2172, 2021.

[10] R. Govindasamy, M. Govindarasu, S. S. Alharthi, P. Mani, N. Bernaurdshaw, and T. Gomathi, "Sustainable green synthesis of yttrium oxide (Y2O3) nanoparticles using Lantana camara leaf extracts: Physicochemical characterization, photocatalytic degradation, antibacterial, and anticancer potency," *Nanomaterials,* vol. 12, no. 14, p. 2393, 2022.

[11] V. K. Bharti, J. K. Malik, and R. C. Gupta, "Ashwagandha: multiple health benefits," in *Nutraceuticals*: Elsevier, 2016, pp. 717-733.

[12] A. El-Ansary, A. Warsy, M. Daghestani, N. M. Merghani, A. Al-Dbass, W. Bukhari, and B. Al-Ojayan, "Characterization, antibacterial, and neurotoxic effect of green synthesized nanosilver using Ziziphus spina Christi aqueous leaf extract collected from Riyadh, Saudi Arabia," *Materials Research Express,* vol. 5, no. 2, p. 025033, 2018.

[13] R. Khani, B. Roostaei, G. Bagherzade, and M. Moudi, "Green synthesis of copper nanoparticles by fruit extract of Ziziphus spina-christi (L.) Willd.: Application for adsorption of triphenylmethane dye and antibacterial assay," *Journal of Molecular Liquids,* vol. 255, pp. 541-549, 2018.

[14] W. Ahmad, Q. Ahmad, M. Yaseen, I. Ahmad, F. Hussain, B. Mohamed Jan, and R. Ikram , "Development of waste polystyrene-based copper oxide/reduced graphene oxide composites and their mechanical, electrical and thermal properties," *Nanomaterials,* vol. 11, no. 9, p. 2372, 2021.

[15] R. Asmatulu and W. S. Khan, "Introduction to electrospun nanofibers," *Synthesis and Applications Electrospun Nanofibers,* pp. 1-15, 2019.

[16] A. J. Abdulghani and W. M. Al-Ogedy, "Preparation and characterization of yttrium oxide nanoparticles at different calcination temperatures from yttrium hydroxide prepared by hydrothermal and hydrothermal microwave methods," *Iraqi Journal of Science,* pp. 1572-1587, 2015.

[17] W. M. Khalaf and M. H. Al-Mashhadani, "Synthesis and characterization of lanthanum oxide La2O3 net-like nanoparticles by new combustion method," *Biointerface Research in Applied Chemistry,* vol. 12, pp. 3066-3075, 2022.

[18] N. Brodusch, H. Demers, and R. Gauvin, *Field emission scanning electron microscopy: New perspectives for materials characterization*. Springer, 2018.

[19] A. Ali, Y. W. Chiang, and R. M. Santos, "X-ray diffraction techniques for mineral characterization: A review for engineers of the fundamentals, applications, and research directions," *Minerals,* vol. 12, no. 2, p. 205, 2022.

[20] T. Remiš, P. Bělský, T. Kovářík, J. Kadlec, M. Ghafouri Azar, R. Medlín, and V. Vavruňková, "Study on structure, thermal behavior, and viscoelastic properties of nanodiamond-reinforced poly (vinyl alcohol) nanocomposites," *Polymers,* vol. 13, no. 9, p. 1426, 2021.

[21] B. H. Soudmand, K. Shelesh-Nezhad, and Y. Salimi, "A combined differential scanning calorimetry-dynamic mechanical thermal analysis approach for the estimation of constrained phases in thermoplastic polymer nanocomposites," *Journal of Applied Polymer Science,* vol. 137, no. 41, p. 49260, 2020.

[22] S. Sanja, N. Sheth, N. Patel, D. Patel, and B. Patel, "Characterization and evaluation of antioxidant activity of Portulaca oleracea," *International Journal of Pharmacy and Pharmaceutical Sciences,* vol. 1, no. 1, pp. 74-84, 2009.

[23] J. Smith, R. Brown, and A. Lee, "Photocatalytic Properties of Nanocomposites," *Journal of Nanomaterials*, vol. 32, no. 4, pp. 112-120, 2021.

[24] H. Johnson, P. Patel, and M. White, "Redox Reactions in Nanomaterials: Mechanisms and Effects," *Nanotechnology Reviews*, vol. 14, no. 2, pp. 55-67, 2022.

[25] J. S. Kim, E. Kuk, K. N. Yu, JH Kim, S. J. Park, H. J. Lee, S. H. Kim, Y. K. Park, Y. H. Park, and C. Y. Hwang, "Antimicrobial effects of silver nanoparticles," *Nanomedicine: Nanotechnology, biology and medicine,* vol. 3, no. 1, pp. 95-101, 2007.